Materials Chemistry and Physics 114 (2009) 145–150

Contents lists available at ScienceDirect

Materials Chemistry and Physics

journal homepage: www.elsevier.com/locate/matchemphys

The effects of alumina nanoparticle on the properties of an epoxy resin system

Abdollah Omrani [a,*], Leonardo C. Simon [b], Abbas A. Rostami [a]

[a] Faculty of Chemistry, University of Mazandaran, P.O. Box 453, Babolsar, Mazandaran, Iran
[b] Department of Chemical Engineering, University of Waterloo, 200 University Avenue West, Waterloo, ON N2L 3G1, Canada

ARTICLE INFO

Article history:
Received 14 June 2008
Received in revised form 27 August 2008
Accepted 29 August 2008

Keywords:
Composite materials
Differential scanning calorimetry (DSC)
Electron microscopy (SEM)
Thermal properties

ABSTRACT

The aim of this investigation is to determine the reinforcing effects of alumina nanoparticle in a diglycidyl ether of bisphenol A (DGEBA) type epoxy resin using different approaches based on *in situ* Fourier transform infrared spectroscopy, differential scanning calorimetry (DSC), dynamic mechanical, mechanical and microstructure measurements. From the kinetic analysis using the Avrami equation, it has been seen that the kinetic parameters are influenced by the presence of nanoparticle and the used curing temperatures. Differential scanning calorimetry was used to probe the changes in reactivity by analyzing the reaction heat and the glass transition temperature values of the cured composites owing to the presence of nanoparticle and due to the diamine hardener. It was also found that a relatively low concentration of Al_2O_3 nanoparticle led to an impressive improvement of dynamic mechanical, mechanical, and thermal properties. The scanning electron microscopy (SEM) photographs showed that the surface roughness increased with the addition of nanoalumina.

1. Introduction

The growing demand to nanomaterials is due to the fact that new chemical and physical properties are attainable when nanosized fillers added into polymer matrixes where a single molecule or the same material without nanofiller does not show such an advantages. In the past decades an extensive research activities have been devoted on incorporating polymers with nanoparticles since polymer-based nanocomposites showed much better thermal and mechanical properties compared to the polymer matrixes having micron sized particles [1–3]. This is due to the effect of the unique nature [4,5] of the nanosized filler on the bulk properties of polymer-based nanocomposites [6,7]. There have been few studies on nanocomposite preparation by direct mixing of nanoparticles and the resin matrix especially for the thermosetting resins. So, knowledge about this issue and what can or cannot be accomplished by it is incomplete yet. Epoxy resins are thermosetting materials that require a cure treatment to attain suitable physical and mechanical properties for industrial applications. Modification of epoxy resins is still necessary since some application in the engineering area require higher mechanical and thermal properties.

Incorporation of various reinforced nanosized phases into epoxy resin is one of the ways to meet the problem with success [8,9]. Different types of nanoparticles such as graphite nanofiber, carbon nanotubes, nanoclays, cellulose nanofiber, and nanoalumina have been utilized to enhance the epoxy rein properties [10–15]. Epoxy resin reinforced with silica particles having submicron dimension represents one of the most studied systems [16,17]. It is generally agreed that the large surface to volume ratio of the nanoscale incorporations plays a key role on the mechanical property improvement [18]. Two concepts are presented in the literature on reinforcement mechanism. One assumes that the formation of a nanostructure network of finely dispersed particles, which are strongly bonded to the polymer, is probably responsible for the reinforcement. In the other concept, the presence of an interphase is integrated into a mechanical-based method to describe the observed reinforcement in composites [19].

In the present study an attempt has been aimed at clarifying the effects of nanoalumina on the kinetics, thermal, dynamic mechanical, and microstructure properties of diglycidyl ether of bisphenol A (DGEBA) type epoxy resin cured with an aliphatic diamine, i.e. diethylentriamine (Dien).

2. Experimental

2.1. Materials and preparation of hybrid samples

Alumina particles (M_w = 101.96 g mol^{-1} in gamma phase) with an average size of 50 nm having a surface area of 35–43 m^2 g^{-1} were purchased from ALDRICH. The epoxy used was diglycidyl ether of bisphenol A with an average $M_n \sim 377$ and viscosity of 100–150 poise at 25 °C purchased from SIGMA–ALDRICH Canada. The epoxy equivalent weight (eew) of the resin and the density at 25 °C were 185 g eq^{-1} and 1.16 g ml^{-1}, respectively. The curing agent was diethylentriamine (M_w = 103.17 g mol^{-1}) in reagent grade with density of 0.955 g ml^{-1} at 25 °C provided

* Corresponding author. Tel.: +98 11252 42025; fax: +98 11252 42002.
E-mail address: omrani@umz.ac.ir (A. Omrani).

0254-0584/$ – see front matter © 2008 Elsevier B.V. All rights reserved.
doi:10.1016/j.matchemphys.2008.08.090

by SIGMA–ALDRICH Canada. A known amount of alumina nanoparticles was added to 5 g of DGEBA at 70 °C to reduce the resin viscosity and then thoroughly stirred on a magnetic stirrer for 10 min to produce homogeneous blends. A stoichiometry value of the aliphatic amine is added into the blends at room temperature. The resulted mixtures were stirred for 5 min by hand mixing treatment and finally kept under liquid nitrogen being undergoes the measurements. About 4–5 mg of the freshly prepared composites was used for the calorimetry measurements. Samples for the dynamic mechanical thermal analysis (DMTA) and flexural tests are prepared by pouring the epoxy composites into a preheated Teflon mold and finally cured 2 h into a vacuum oven at 80 °C.

2.2. Characterization techniques

Differential scanning calorimetry (DSC) measurements were performed with a TA Q100 calorimeter using nitrogen atmosphere. The samples were heated in the temperature range of −30 and 300 °C at a heating speed of 20 °C min^{-1} and then cooled to −30 °C to minimize the enthalpy relaxation. Finally, the samples were reheated to 250 °C at 20 °C min^{-1} to determine the glass transition temperature (T_g) of the fully cured composites. DMTA studies of the both neat and nanoalumina/epoxy/amine composites are carried out on a model DMTA V dynamic mechanical analyzer (Rheometric Scientific). All samples were tested using a sample size of (15 mm × 5 mm × 1 mm) under single cantilever mode. The temperature rang varied from 35 °C to above the T_g of fully cured materials at a heating speed of 5 °C min^{-1} at frequency of 1 Hz.

A FE-SEM 1530 from LEO was used to probe the dispersion of nanoalumina on the fracture surfaces of the cured composites. The fracture surface were gold coated prior to scanning electron microscopy (SEM) studies to avoid charging and were examined at 15 kV accelerating voltage. FT-IR experiments are examined on the samples between two KBr pellets inside the Bruker Tensor 27 spectrometer. Each spectrum was scanned 32 times at a resolution of 4 cm^{-1} from 400 to 4000 cm^{-1}. Spectra are monitored and analyzed by OPUS software. The flexural and tensile properties of the epoxy with and without nanoalumina are determined on samples with approximately dimensions of 25 mm × 5 mm × 1 mm using a MiniMat 2000 mechanical testing machine. Five tests are conducted on each sample according to ASTM D-790-93 method and a crosshead speed of 2 mm min^{-1} is employed.

3. Results and discussion

3.1. Calorimetery studies

The curing reaction of the epoxy compositions was investigated by means of DSC. Fig. 1 compares the DSC thermograms of the cured epoxy and its composites. The decrease of the temperature of the curing peaks with increasing concentration of alumina particle for the system indicates the catalytic effect of the filler on epoxy cure. The peak maximum is shifted towards the lowest temperatures for the composite having 5 phr of the nanofiller. Further analysis of the DSC thermograms exhibit that the reaction heat of DGEBA/Dien system included 0.5 phr of the filler is higher than that of the neat

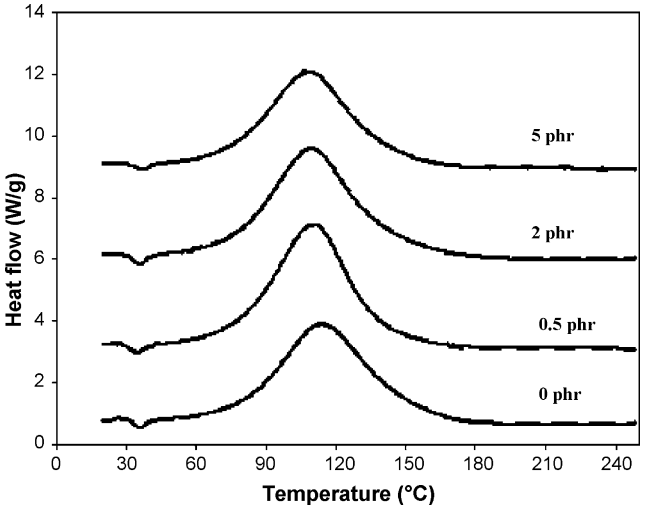

Fig. 1. Calorimetric tests on DGEBA/Dien and DGEBA/Dien/nanoalumina composites under dynamic conditions.

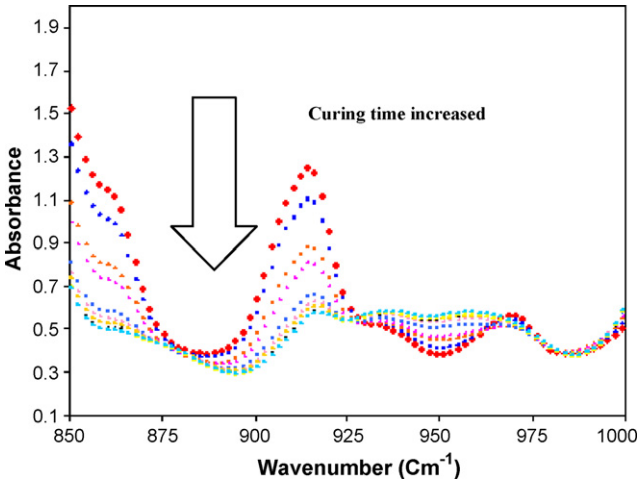

Fig. 2. Spectra from FT-IR measurements on DGEBA/Dien/nanoalumina (2 phr) composite cured at 90 °C at various time.

resin and then decreases with increasing concentration. The value of reaction enthalpy is found to be 521, 553, 549, and 486 J (gr-epoxy)$^{-1}$ for the 0, 0.5, 2, and 5 phr level of the filler concentration, respectively. This means that high level of nanoalumina loading has a converse effect on the polymer network formation. It could be described by topological restrictions produced during the epoxy network evolution. The T_g of the cured compositions having 0, 0.5, 2, and 5 phr of the nanoalumina particles is also determined to be 88, 114, 112, 105 °C, respectively. However, the addition of the alumina nanoparticle increases T_g by about 17–26 °C in comparison with T_g of neat epoxy resin.

That confirms the polymer chains must be under constraint because of the influence of the interfacial–particle interactions.

3.2. Cure kinetics

Kinetics of the studied cure reactions is investigated under isothermal conditions by analyzing the spectra obtained by means of FT-IR instrument. The method was based on exploring reduce in the peak area of the epoxy group vibration at 915 cm^{-1} with time.

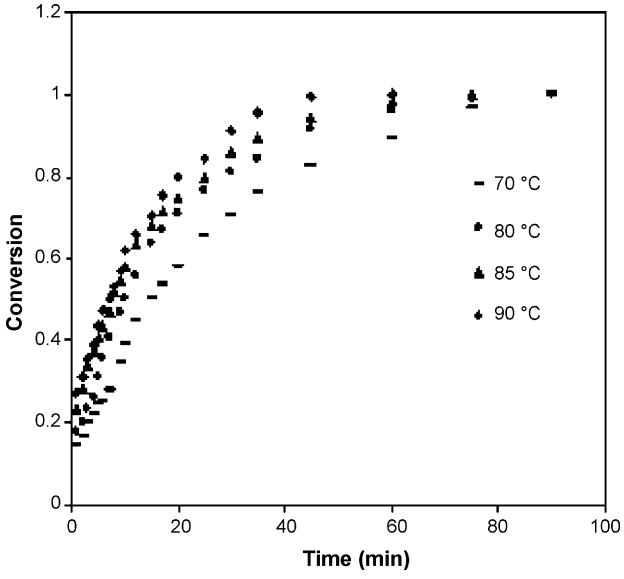

Fig. 3. Conversion of epoxide groups versus time plots for DGEBA/Dien/nanoalumina (0.5 phr) at different isothermal temperatures.

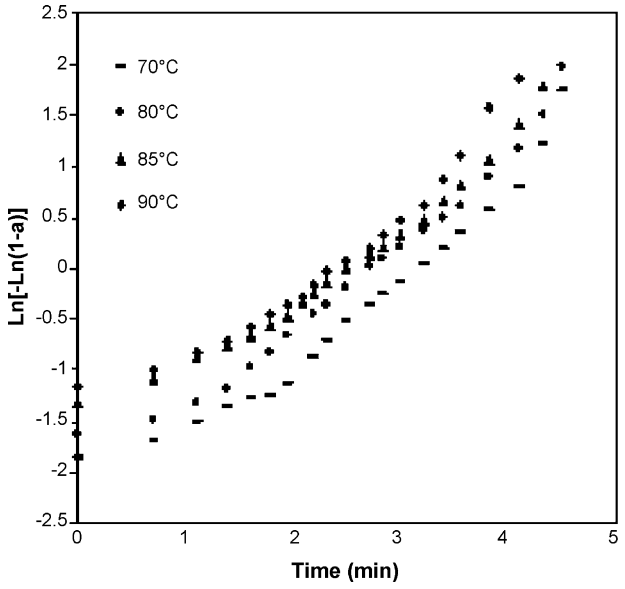

Fig. 4. Representative plots obtained using the Avrami equation to determine n and k for DGEBA/Dien/nanoalumina (0.5 phr) composite at different isothermal temperatures.

The degree of conversion is calculated by normalizing epoxy group vibration with the absorbance bond at 1509 cm^{-1}. Isothermal temperatures of 70, 80, 85, and 90 °C are imposed on the Dien-based composites. Representative IR curves of the epoxy involved 2 phr nanoalumina cured at 90 °C are displayed in Fig. 2. From the FT-IR spectra the degree of conversion for epoxide group calculated and the representative result for the composite having 2 phr nanoalumina is shown in Fig. 3. The modified Avrami equation [20,21], is used to estimate the kinetic parameters of cure. Using the Avrami equation (Eq. (1)) and its double logarithmic form (Eq. (2)) the kinetic parameters, the exponent n and the rare constant k, for the epoxy and its composites could be obtained:

$$1 - \alpha_t = \exp(-kt^n) \quad (1)$$

$$\mathrm{Ln}[-\mathrm{Ln}(1-\alpha_t)] = \mathrm{Ln}\,k + n\,\mathrm{Ln}\,t \quad (2)$$

where α_t is the relative degree of epoxide conversion for time t and n is the order of reaction. A plot of the left side of Eq. (2) in terms of Ln t allows estimating the key parameters of cure kinetics, n and k from the slope and intercept, respectively. Representative plots of $\mathrm{Ln}[-\mathrm{Ln}(1-\alpha_t)]$ versus $\mathrm{Ln}(t\,\mathrm{min}^{-1})$ for the composite having 0.5 phr of nanoalumina is shown in Fig. 4.

It should be noted that the kinetic parameters do not have the same meaning in the isothermal and non-isothermal curing because of the fact that under dynamic heating the temperature changes constantly and affects the rates of both microgels formation and its growth. The obtained data are presented in Table 1. As it is seen in Table 1, the curing rate constants are appeared to be related to the isothermal temperatures and the filler concentration. The values of k have a shift to higher values with increasing curing temperature. Further, at the same given temperature, the values of the cure rate constants augment with the addition of nanoalumina. The exponent n of DGEBA/Dien-based composites varied between 0.71 and 0.82. The Avrami exponent of n is known to be influenced by molecular weight, nucleation type, and in general is not much influenced by temperature.

Table 1
Avrami kinetic parameters of reaction rate constants and reaction orders from FT-IR data

System	Al_2O_3 (phr)	Temperature (°C)	n	k (s^{-1})
DGEBA/Dien	0	70	0.88	0.0473
DGEBA/Dien	0	80	0.90	0.0678
DGEBA/Dien	0	85	0.89	0.0797
DGEBA/Dien	0	90	0.74	0.1590
DGEBA/Dien	0.5	70	0.79	0.088
DGEBA/Dien	0.5	80	0.81	0.1163
DGEBA/Dien	0.5	85	0.72	0.1798
DGEBA/Dien	0.5	90	0.75	0.1896
DGEBA/Dien	2	70	0.80	0.0591
DGEBA/Dien	2	80	0.74	0.0844
DGEBA/Dien	2	85	0.73	0.0993
DGEBA/Dien	2	90	0.77	0.1187
DGEBA/Dien	5	70	0.82	0.0635
DGEBA/Dien	5	80	0.78	0.0860
DGEBA/Dien	5	85	0.73	0.1140
DGEBA/Dien	5	90	0.71	0.1430

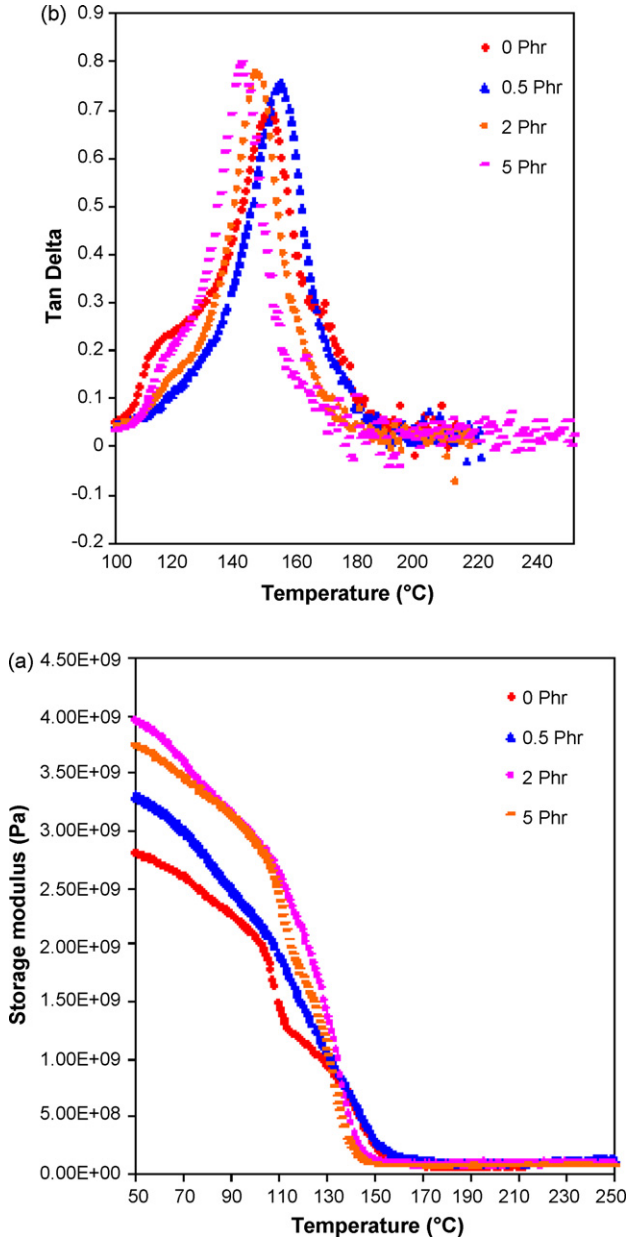

Fig. 5. DMTA results of neat epoxy and its composites. (a) Storage modulus and (b) Loss factor (tan δ).

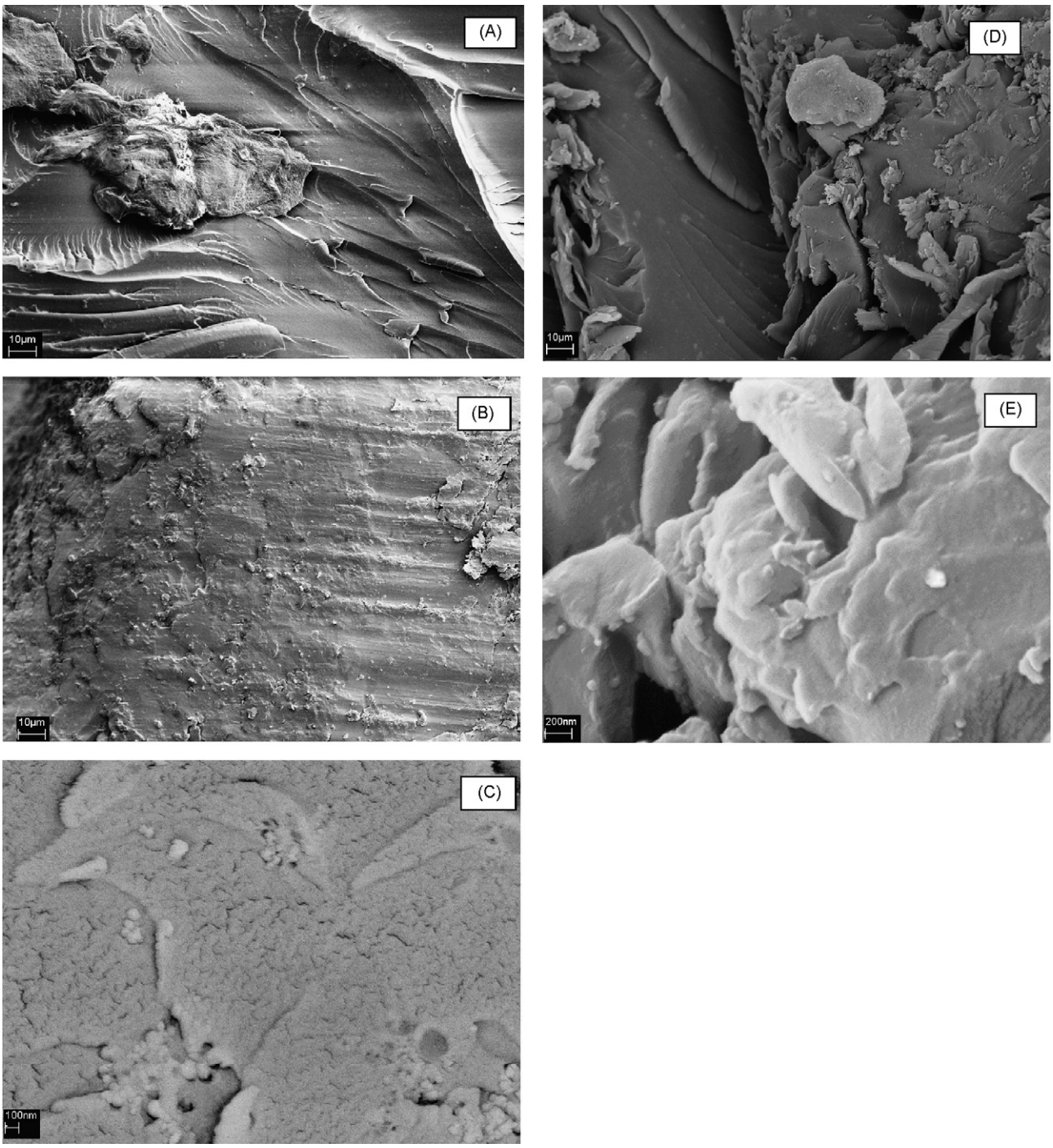

Fig. 6. SEM images on fracture surface of neat epoxy and its composites at various magnifications of low (1k×), medium (10k×) and high (50k×). (A) Without filler and medium magnification, (B) 0.5 phr and low magnification, (C) 0.5 phr and high magnification, (D) 5 phr and low magnification, and (E) 5 phr and high magnification.

3.3. Viscoelastic properties

The effect of nanoalumina on the viscoelastic properties of crosslinked polymers has been probed using DMTA in the temperature range of 35–250 °C. This technique allows to investigate the α relaxation related to the Brownian motion of the main chains due to the transitions occurred during the cure process. It is likely that this motion can be affected by nanoalumina because of interactions in the interface layer around the particles. Fig. 5 shows the temperature dependency of storage modulus and $\tan\delta$ of the neat epoxy and it composites. As it is shown in Fig. 5, the presence of the nanofiller with 0.5–5 phr concentration enhances the values of storage modulus and this effect appear to be different in magnitude at various temperature range depend on the initial epoxy compositions. Clearly, it may be confirmed that the amplitude of storage modulus in the rubbery plateau region increases with increasing the filler loading up to 2 phr. At high concentration of 5 phr nanoalumina, it is considered that the filler is dispersed into the epoxy matrix irregularly and the void of the cross-linking is increased. Then the segmental mobility rises, which leads to the decrease of the storage modulus at the same temperature range.

Fig. 5 also exhibit that the tan δ peak area decreases and becomes broader with increasing nanofiller content, and this indicates that the chain mobility of the crosslinked epoxy is restricted by the presence of nanoalumina. The reduction in tan δ peak is consistent with the increase in T_g as it is seen in the DSC measurements. This may be described according to an interface layer effect due to chains being tied down by the surface of nanoalumina at low level of loading. In addition, when the nanoalumina loading being up to 2 or 5 phr, the T_g decreased as well. However, the main important factors that can affect T_g are degree of particle dispersion and curing conditions.

3.4. Fractography

SEM analysis was carried out on the fracture surface of neat epoxy and its composites having 0.5, 2 and 5 phr nanofiller to qualitatively evaluate the particle–matrix interface and evidence the eventual presence of particle aggregations. The fracture surface of the neat epoxy reveals a brittle behavior characterized by large smooth area which corresponds to the low growth of crack like defects. As it can be seen in Fig. 6, the state of dispersion was approximately well and a suitable adhesion between alumina particles and the resin matrix have been attained at low level of loading 0.5 phr. The bright spots on the back-scattered images correspond to alumina aggregates. A considerable aggregation of particles is observed at high level of loading 5 phr as evidenced by the presence of large voids around the particle aggregates. Apparently, a portion of the filler remains at the microscale level with different size population which, of course, is depending on the mixing conditions and epoxy compositions. It may be implied that the conventional mixing was not able to completely break up the agglomerates for achieving a homogeneous dispersion. At high nanoalumina content, a preventive surface treatment of the particle could be useful to obtain complete deagglomeration. It seems that the cohesion of the alumina particles and the viscosity of the resin might prevent the uniform dispersion.

In the magnified images of the particle–matrix parts, the resin besieged the particles. It is clear that the crack usually initiates from where surface defects or high stress regions could be observed. Therefore, it is interesting to see that the matrix has diffused deeply inside the aggregate to divide it into smaller stacks at low level of loading but these microcracks jointed together to form a single dominant crack and the final failure of the specimen will be occurred by microvoid coalescence at high level of loading which is responsible for the weak mechanical properties (see Section 3.5).

3.5. Mechanical properties

Tensile and flexural properties of epoxy and its composites are determined, and since they behave in a similar trend, only the flexural properties are depicted in Fig. 7. The load versus the deflection of the specimens at the midpoint is recorded and then flexural modulus has been calculated. The relationship between the flexural modulus and the nanoalumina content is shown in Fig. 7. It is clear that the addition of nanoalumina results in an increase in modulus at low level of loadings 0.5 and 2 phr. This may be due to more effectively swell of the filler in the resin matrix leading to reliable dispersion and lager stiffness. On likely, explanation for this good reinforcement effect is the increase in effective volume fraction of reinforcement entities as the distance between the filler increased. When the level of loading was over 2 phr, the flexural modulus is decreased.

It is believed that the aggregation of nanoparticles at high concentration of 5 phr is responsible for the low value of flexural modulus. However, the flexural modulus of the neat epoxy and DGEBA/Dien/nanoalumina (2 phr) composite are found to be 2120 and 3526 MPa, respectively.

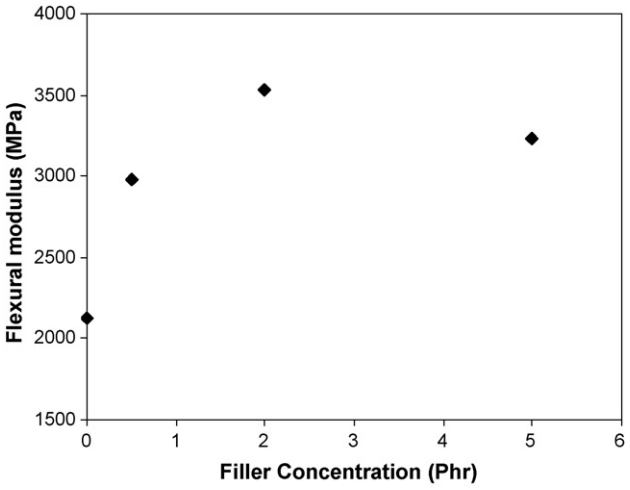

Fig. 7. Flexural properties of neat epoxy and its composites.

4. Conclusions

From this study, we drew the following remarks:

(1) Nanoalumina/epoxy matrix composites have been processed with different nanofiller content up to 5 phr.
(2) The good stabilization of the nanoalumina in the diethylentriamine leads to a good dispersion of the filler especially at low level of loadings.
(3) There is no significant variation in the Avrami exponent of n among the samples. Thus the presence of nanoalumina dose not seem to have tremendous effect on the growing of microgels in the system during curing.
(4) The DMA showed increased storage modulus and T_g with increased the nanoparticle concentration.
(5) Although, the dispersion of nanoalumina was not perfectly homogeneous, incorporation of the filler results in higher fracture toughness by crack deviation because of the presence of nanoparticles.
(6) It can finally be suggested that 0.5 phr nanoalumina/epoxy/diamine composite showed the best balance of viscoelastic and thermal properties due to homogeneous dispersion.

Acknowledgements

The research has been financially supported by the University of Mazandaran and Discovery NSERC-Canada.

References

[1] L.G. Yu, S.R. Yang, H.T. Wang, J. Appl. Polym. Sci. 77 (2000) 2404.
[2] J.-C. Huang, X.-F. Qian, J. Yin, Z.-K. Zhu, H-j. Xu, Mater. Chem. Phys. 69 (2001) 172.
[3] E. Rejhaud, C. Gauthier, J. Perez. Rev. Metall. 96 (1999) 169.
[4] R.F. Service, Science 249 (5546) (2001) 1448.
[5] S. Auer, D. Frenkel, Nature 413 (6857) (2001) 711.
[6] Z.K. Zhu, Y. Yang, J. Yin, J. Appl. Polym. Sci. 73 (1999) 2977.
[7] T. Agag, T. Koga, T. Takeichi, Polymer 42 (2001) 3399.
[8] S. Chand, J. Mater. Sci. 35 (2000) 1303.
[9] M. Krumova, C. Klingshirn, F. Haupert, K. Friedrich, Compos. Sci. Technol. 61 (2001) 557.
[10] A.A. Cooper, R.J. Young, M. Halsall, Compos. Part A: Appl. Sci. Manuf. 32 (2001) 401.

[11] G.Z. Chen, M.S.P. Shaffer, D. Coleby, G. Dixon, W. Zhou, A.H. Windle, Adv. Mater. 12 (2000) 522.
[12] J. Sandler, T.P. Schaffer, W. Bauhofer, K. Schulte, A.H. Windle, Polymer 40 (1999) 5967.
[13] A. Omrani, L.C. Simon, A.A. Rostami, Mater. Sci. Eng. Part A 490 (2008) 131.
[14] N. Shanid, R.G. Villate, A.R. Barron, Compos. Sci. Technol. 65 (2005) 2250.
[15] E.N. Gilbert, B.S. Hayes, J.C. Seferis, Polym. Eng. Sci. 43 (5) (2003) 1096.
[16] Y. Zheng, Y. Zheng, R. Ning, Mater. Lett. 57 (2003) 2940.
[17] Y.-L. Liu, C.-Y. Hsu, W.-L. Wei, R.-J. Jeng, Polymer 44 (2003) 5159.
[18] K. Friedrich, K. Karson, Fiber Sci. Technol. 18 (1983) 34.
[19] N.S. Enikolopyan, M.L. Fridman, I.O. Stalnova, V.L. Popov, Adv. Polym. Sci. 96 (1990) 1.
[20] W. Xu, S. Bao, S. Shen, W. Wang, G. Hang, P. He, J. Polym. Sci. Part B: Polym. Phys. 41 (2003) 378.
[21] D.Z. Chen, P.S. He, L.J. Pan, Polym. Test. 22 (2003) 689.